

# UC Berkeley

## UC Berkeley Previously Published Works

### Title

Measuring chirality in NMR in the presence of a time-dependent electric field

### Permalink

<https://escholarship.org/uc/item/9ht7f086>

### Journal

The Journal of Chemical Physics, 140(23)

### ISSN

0021-9606

### Authors

Walls, Jamie D  
Harris, Robert A

### Publication Date

2014-06-21

### DOI

10.1063/1.4882698

### Copyright Information

This work is made available under the terms of a Creative Commons Attribution License, available at <https://creativecommons.org/licenses/by/4.0/>

Peer reviewed

# Measuring chirality in NMR in the presence of a time-dependent electric field

Jamie D. Walls<sup>1,a)</sup> and Robert A. Harris<sup>2</sup>

<sup>1</sup>Department of Chemistry, University of Miami, Coral Gables, Florida 33124, USA

<sup>2</sup>Department of Chemistry, University of California, Berkeley, Berkeley, California 94720, USA

(Received 21 March 2014; accepted 29 May 2014; published online 16 June 2014)

Traditional nuclear magnetic resonance (NMR) experiments are “blind” to chirality since the spectra for left and right handed enantiomers are identical in an achiral medium. However, theoretical arguments have suggested that the effective Hamiltonian for spin-1/2 nuclei in the presence of electric and magnetic fields can be different for left and right handed enantiomers, thereby enabling NMR to be used to spectroscopically detect chirality even in an achiral medium. However, most proposals to detect the chiral NMR signature require measuring signals that are equivalent to picomolar concentrations for <sup>1</sup>H nuclei, which are outside current NMR detection limits. In this work, we propose to use an AC electric field that is resonantly modulated at the Larmor frequency, thereby enhancing the effect of the chiral term by four to six orders of magnitude. We predict that a steady-state transverse magnetization, whose direction will be opposite for different enantiomers, will build up during application of an AC electric field. We also propose an experimental setup that uses a solenoid coil with an AC current to generate the necessary periodic electric fields that can be used to generate chiral signals which are equivalent to the signal from a <sup>1</sup>H submicromolar concentration. © 2014 AIP Publishing LLC. [<http://dx.doi.org/10.1063/1.4882698>]

## I. INTRODUCTION

The nuclear magnetic resonance (NMR) spectra for right and left handed molecules in an achiral medium are identical. As such, NMR is “blind” to chirality, and the only experimentally demonstrated methods to observe differences between left and right handed molecules using NMR have been to create effective diastereomers using, for example, chiral shift reagents or by recording the spectrum in a chiral medium.<sup>1</sup>

In 2004, however, Buckingham<sup>2</sup> proposed that NMR, in combination with an electric field, could be used to distinguish between left and right handed molecules in achiral environments. For a single spin-1/2 particle in the presence of static magnetic and electric fields, the Hamiltonian can be written as the normal Zeeman interaction along with a pseudoscalar contribution that changes sign for right and left handed molecules:

$$\frac{\hat{H}}{\hbar} = -(1 - \sigma)\gamma\vec{B} \cdot \vec{\hat{S}} + \sigma_c\gamma\vec{B} \times \vec{E} \cdot \vec{\hat{S}}, \quad (1)$$

where  $\vec{\hat{S}}$  are spin-1/2 operators,  $\gamma$  is the nuclear gyromagnetic ratio,  $\sigma$  is the dimensionless isotropic chemical shielding constant ( $\sigma$  is on the order of 1–10 ppm for <sup>1</sup>H), and  $\sigma_c$  (dimensions of  $\frac{m}{V}$ ) is the pseudoscalar chemical shielding polarizability constant, which is zero for achiral molecules and has opposite sign for right (R) and left (L) handed molecules, i.e.,  $(\sigma_c)_L = -(\sigma_c)_R$ . A simple derivation of the form of  $\hat{H}$  in Eq. (1) based upon symmetry arguments was also provided by Harris and Jameson.<sup>3</sup>

In this case, measuring the signal proportional to  $\sigma_c$  provides a signed measurement that can be used to distinguish between left and right handed molecules.<sup>2,4–6</sup> Quantum chemical calculations by Buckingham and Fischer<sup>4</sup> predicted that  $|\sigma_c| \approx 2 \times 10^{-18} \frac{m}{V}$  for <sup>1</sup>H and  $|\sigma_c| \approx 2 \times 10^{-17} \frac{m}{V}$  for <sup>19</sup>F in chlorofluoroacetic acid CHClF(COOH). Recently, a  $|\sigma_c|$  an order of magnitude larger was predicted by Monaco and Zanasi<sup>7</sup> for 8,9-difluoro-*P*-hexahelicene, where  $|\sigma_c| \approx 1.5 \times 10^{-16} \frac{m}{V}$  for <sup>19</sup>F. Note that for molecules with a permanent electric dipole moment, the magnitude of  $\sigma_c$  in Eq. (1) can be enhanced by two to three orders of magnitude.<sup>6</sup>

However, measuring the “chiral” signal for such small values of  $\sigma_c$  is outside current NMR detection limits, which are on the order of  $\mu\text{M}$  concentrations<sup>8</sup> for <sup>1</sup>H, although recent work in nuclear hyperpolarization can potentially lower this detection limit by a few orders of magnitude.<sup>9</sup> To understand where the difficulty of such measurements arises, consider the case where the large, static magnetic and electric fields are applied in the  $\hat{z}$ - and  $\hat{y}$ -directions, respectively, i.e.,  $\vec{B} = |\vec{B}|\hat{z}$  and  $\vec{E} = |\vec{E}|\hat{y}$ . The Hamiltonian in Eq. (1) can then be written as

$$\frac{\hat{H}}{\hbar} = -(1 - \sigma)\omega_Z\hat{S}_Z - \sigma_c|\vec{E}|\omega_Z\hat{S}_X, \quad (2)$$

where  $\omega_Z = \frac{\gamma|\vec{B}|}{\hbar}$  is the Larmor frequency. In this case,  $\hat{H}$  in Eq. (2) is equivalent to a spin-1/2 interacting with a static magnetic field,  $\vec{B}_{\text{eff}}$ , given by  $\frac{\gamma\vec{B}_{\text{eff}}}{\hbar} = -(1 - \sigma)\omega_Z\hat{z} - \sigma_c|\vec{E}|\omega_Z\hat{x}$ , where  $-(1 - \sigma)\omega_Z\hat{z}$  represents the large static Zeeman field, and  $-\sigma_c|\vec{E}|\omega_Z\hat{x}$  represents the effective transverse magnetic field due to the chiral contribution to  $\hat{H}$  in Eq. (2). For a large static electric field of  $|\vec{E}| = 10^6 \frac{V}{m}$ , the

<sup>a)</sup> Author to whom correspondence should be addressed. Electronic mail: [jwalls@miami.edu](mailto:jwalls@miami.edu)

effective strength of the transverse component of  $\vec{B}_{\text{eff}}$  is approximately  $|\sigma_c \vec{E}| = 2 \times 10^{-12}$  smaller than the longitudinal component of  $\vec{B}_{\text{eff}}$  for  $^1\text{H}$ . In this case, the equilibrium magnetization is tilted away from the  $\hat{z}$ -direction<sup>5</sup> by an angle  $\theta$  such that  $|\sin(\theta)| \approx |\theta| \approx \frac{|\sigma_c \vec{E} \omega_Z|}{\sqrt{(\sigma_c |\vec{E}| \omega_Z)^2 + (\omega_Z)^2}} \approx |\sigma_c \vec{E}| \approx 2 \times 10^{-12}$  for  $^1\text{H}$ . Different handed molecules will tilt the magnetization in opposite directions  $[(\theta)_L = -(\theta)_R]$ , and hence measuring the direction of the small tilting of the magnetization provides a method that discriminates left and right handed enantiomers using NMR.<sup>2,4,5</sup> However, assuming that the concentration of the molecules are on the order of 1 M, the chiral signal that is generated under crossed magnetic and electric fields in Eq. (2) is equivalent to the signal from a picomolar solution, which, as stated above, is outside current NMR detection limits.

The chiral contribution to  $\hat{H}$  in Eq. (2),  $\sigma_c |\vec{E}| \omega_Z$ , acts like a static, transverse magnetic field along the  $\hat{x}$ -direction that is approximately  $10^{-12}$  times smaller than the static Zeeman field, which results in minimal tilting of the magnetization along the  $\hat{z}$ -direction as described above. In NMR, however, small, radiofrequency (RF) magnetic fields, with strengths ranging from Hz to tens of kHz, are routinely used in liquid-state NMR to generate highly nonlinear excitations ( $\theta \gg \frac{\pi}{3}$ ) by modulating the RF fields at the Larmor frequency,  $\omega_Z = \frac{\gamma |\vec{B}|}{\hbar}$ . This suggests that the effects of the chiral contribution to  $\hat{H}$  in Eq. (2) can be enhanced by using a time-dependent electric field that is periodically modulated at  $\omega_Z$ . In this work, we examine the spin dynamics under a periodically driven electric field,  $\vec{E}(t) = E_{\text{amp}} \sin(\omega_r t) \hat{y}$  in Eq. (2), and predict that the chiral signal can be enhanced by four to six orders of magnitude for  $^1\text{H}$ , thereby placing the observation of the chiral signal within the NMR detection limits. We also propose an experimental setup to generate the necessary periodic electric fields while minimizing the effects of the displacement magnetic field<sup>10</sup> that are a consequence of a time-dependent electric field. Finally, simple numerical simulations are provided that support our proposal.

## II. SPIN DYNAMICS UNDER A TIME-DEPENDENT ELECTRIC FIELD

For simplicity, we take the electric field to be time-dependent and given by  $\vec{E}(t) = E_{\text{amp}} \sin(\omega_r t) \hat{y}$  (the actual form will depend upon the experimental setup). In this case, the Hamiltonian in Eq. (2) will simply depend parametrically on  $\vec{E}$  and can be written as

$$\frac{\hat{H}(t)}{\hbar} = -(1 - \sigma) \omega_Z \hat{S}_Z - \sigma_c E_{\text{amp}} \sin(\omega_r t) \omega_Z \hat{S}_X. \quad (3)$$

Two assumptions were made in writing Eq. (3). First, it was assumed that the time-dependent electric field does not affect  $\sigma_c$ , and that modulating the electric field simply modulates  $\hat{H}(t)$  parametrically. This assumption can be justified<sup>12</sup> as long as  $\omega_r$  is modulated at frequencies much smaller than any electronic and/or vibrational transition frequency between electronic and vibrational states that determine  $\sigma_c$ , which is satisfied for currently available  $^1\text{H}$  Larmor frequencies examined in this work,  $\frac{\omega_Z}{2\pi} \in (0.5, 1 \text{ GHz})$ . The second and

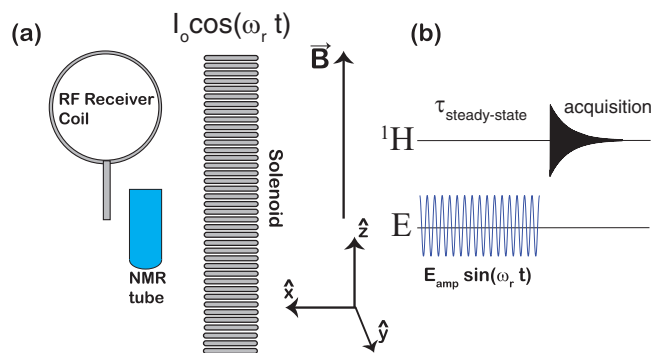


FIG. 1. (a) Schematic for the experimental setup to observe the effects of the pseudoscalar chemical shielding polarizability constant,  $\sigma_c$  in Eq. (1), using crossed electric and magnetic fields. The experiment is performed in a large static magnetic field,  $\vec{B} = |\vec{B}| \hat{z}$ . A long (infinite), tightly wound solenoid (radius  $a$  with  $n$  windings/m) with a time-dependent current,  $I(t) = I_0 \cos(\omega_r t)$ , will generate an oscillating electric field outside the solenoid in the  $xy$ -plane along with an oscillating magnetic field along the  $\hat{z}$ -direction.<sup>11</sup> Taking the central axes for the NMR tube and solenoid to lie within the  $xz$ -plane, the sample in the NMR tube will experience a periodic electric field along the  $\hat{y}$ -direction. An RF receiver coil is used to detect the steady-state transverse magnetization that is generated by the time-dependent electric field. (b) Proposed experiment to detect  $\sigma_c$ . A time-dependent electric field is applied for a time  $\tau_{\text{steady-state}}$  such that a steady-state magnetization is reached, which is given in Eq. (7). After a time  $\tau_{\text{steady-state}}$ , the electric field is turned off, and the steady-state transverse magnetization is detected. The sign of the signal will be opposite for left and right-handed molecules.

more restrictive assumption is that we can neglect the magnetic field generated from the time-dependent electric field in Eq. (3), i.e., the magnetic field resulting from the displacement current<sup>10</sup> can be neglected. In order to justify this assumption, the time-dependent displacement magnetic field must be along the  $\hat{z}$ -axis, with any transverse component to the displacement magnetic field being much less than  $|\frac{\sigma_c E_{\text{amp}} \omega_Z}{2}|$ . This constraint places strict limitations on any proposed experimental setup to generate the time-dependent electric fields in Eq. (3). One proposed experimental setup to measure  $\sigma_c$  is shown in Fig. 1(a), where the time-dependent electric field is generated by a solenoid coil. Details of this experimental setup are given in Sec. III.

With the above assumptions,  $\hat{H}(t)$  in Eq. (3) can be transformed into the rotating frame defined by  $\hat{V}_{INT}(t) = e^{i\omega_r t \hat{S}_Z}$ . In this interaction frame, the effective Hamiltonian,  $\tilde{H}_{INT}(t)$ , is given by

$$\begin{aligned} \frac{\tilde{H}_{INT}(t)}{\hbar} &= -\frac{i}{\hbar} \hat{V}_{INT}^\dagger(t) \frac{d\hat{V}_{INT}(t)}{dt} + \hat{V}_{INT}^\dagger(t) \frac{\hat{H}(t)}{\hbar} \hat{V}_{INT}(t) \\ &= (\omega_r - (1 - \sigma) \omega_Z) \hat{S}_Z - \frac{\sigma_c E_{\text{amp}} \omega_Z}{2} \hat{S}_Y \\ &\quad + \frac{\sigma_c E_{\text{amp}} \omega_Z}{2} (\cos(2\omega_r t) \hat{S}_Y - \sin(2\omega_r t) \hat{S}_X). \quad (4) \end{aligned}$$

By transforming into the rotating frame, the Hamiltonian in Eq. (4) is similar to the Hamiltonian for a spin in the presence of a static field,  $\frac{\gamma \vec{B}_{INT}}{\hbar} = (\omega_r - (1 - \sigma) \omega_Z) \hat{z} - \frac{\sigma_c E_{\text{amp}} \omega_Z}{2} \hat{y}$ , along with a time-dependent transverse field rotating counterclockwise with a frequency  $2\omega_r$ . If  $\omega_r \approx \omega_Z$ , then the time-dependent rotating transverse field in Eq. (4) can be safely neglected since  $|\sigma_c E_{\text{amp}}| \ll 1$ , and the spin

dynamics is governed by an effective time-independent Hamiltonian in the rotating frame given by

$$\frac{\tilde{H}_{INT}}{\hbar} \approx \Delta\omega \hat{S}_Z - \frac{\sigma_c E_{amp} \omega_Z}{2} \hat{S}_Y, \quad (5)$$

where  $\Delta\omega = \omega_r - (1 - \sigma)\omega_Z$ . By taking  $\omega_r \approx (1 - \sigma)\omega_Z$ ,  $\Delta\omega \ll \omega_Z$ , and the magnitude of the longitudinal component of the effective field in Eq. (5),  $\Delta\omega$ , can be experimentally reduced down to at least the order of one-half the intrinsic spin width,  $|\Delta\omega| \leq \frac{1}{T_2}$ , where  $T_2$  is the spin system's transverse relaxation time constant. Since typical transverse ( $T_2$ ) and longitudinal ( $T_1$ ) relaxation times are on the order of seconds in liquid-state samples, the transverse magnetic field generated by the chiral term in Eq. (5) is still too small to generate any significant nutation of the initial  $\hat{z}$ -magnetization, and the effects of relaxation during evolution under  $\tilde{H}_{INT}$  in Eq. (5) have to be included. This can be accomplished by solving the dynamics of the magnetization in the rotating frame defined by  $\hat{V}_{INT}(t)$ ,  $\vec{M}(t) = \tilde{M}_X(t)\hat{x} + \tilde{M}_Y(t)\hat{y} + \tilde{M}_Z(t)\hat{z}$ , by using the Bloch equations with relaxation:

$$\begin{aligned} \frac{d\tilde{M}_X(t)}{dt} &= \frac{\sigma_c E_{amp} \omega_Z}{2} \tilde{M}_Z(t) + \Delta\omega \tilde{M}_Y(t) - \frac{\tilde{M}_X(t)}{T_2}, \\ \frac{d\tilde{M}_Y(t)}{dt} &= -\Delta\omega \tilde{M}_X(t) - \frac{\tilde{M}_Y(t)}{T_2}, \\ \frac{d\tilde{M}_Z(t)}{dt} &= -\frac{\sigma_c E_{amp} \omega_Z}{2} \tilde{M}_X(t) - \frac{\tilde{M}_Z(t) - M_{eq}}{T_1}, \end{aligned} \quad (6)$$

where  $M_{eq}$  is the magnitude of the equilibrium magnetization in the presence of the Zeeman field.

A steady-state will be reached on time  $\tau_{steady-state} \approx \frac{5T_1 T_2}{T_1 + T_2}$ , such that  $\frac{d\tilde{M}_X(t)}{dt} = \frac{d\tilde{M}_Y(t)}{dt} = \frac{d\tilde{M}_Z(t)}{dt} = 0$  in Eq. (6). The steady-state solutions to Eq. (6) are given by<sup>13</sup>

$$\begin{aligned} \tilde{M}_{X,ss} &= M_{eq} \frac{2\sigma_c E_{amp} \omega_Z T_2}{4 + 4(T_2 \Delta\omega)^2 + (\sigma_c E_{amp} \omega_Z)^2 T_1 T_2}, \\ \tilde{M}_{Y,ss} &= -M_{eq} \frac{2\Delta\omega \sigma_c E_{amp} \omega_Z (T_2)^2}{4 + 4(T_2 \Delta\omega)^2 + (\sigma_c E_{amp} \omega_Z)^2 T_1 T_2}, \\ \tilde{M}_{Z,ss} &= M_{eq} \frac{4 + 4(\Delta\omega T_2)^2}{4 + 4(T_2 \Delta\omega)^2 + (\sigma_c E_{amp} \omega_Z)^2 T_1 T_2}. \end{aligned} \quad (7)$$

In this case, the steady-state, transverse magnetization is proportional to  $\sigma_c$ , which will be opposite for left and right-handed enantiomers, thus providing a signed measurement of handedness using NMR. To get an estimate of the size of the signal, take  $\frac{\omega_Z}{2\pi} = 600$  MHz,  $E_{amp} = 10^2 \frac{V}{m}$ ,  $T_1 = T_2 = 1$  s,  $|\Delta\omega| \approx \frac{1}{T_2}$ , and  $|\sigma_c| = 2 \times 10^{-18} \frac{m}{V}$  for <sup>1</sup>H. In this case,  $|\tilde{M}_{Y,ss}| \approx |\tilde{M}_{X,ss}| \approx 2 \times 10^{-7} M_{eq}$ , which is within the realm of detection using liquid-state NMR. For <sup>19</sup>F NMR, the steady-state transverse magnetization in Eq. (7) can be approximately one to two orders of magnitude greater than the steady-state signal for <sup>1</sup>H.

### III. PROPOSED EXPERIMENTAL SETUP TO DETECT $\sigma_c$

In writing the steady-state magnetization in Eq. (7), the only transverse magnetic field that was assumed to be present

was that generated by the chiral contribution in Eq. (5),  $-\frac{\sigma_c E_{amp} \omega_Z}{2} \hat{y}$ . As a result, the sign of the steady-state transverse magnetization in Eq. (7) could be used to distinguish between right and left-handed enantiomers. As mentioned above, a time-dependent electric field will, as a consequence of Maxwell's equations,<sup>10</sup> generate a time-dependent magnetic field. In this case, the magnitude of the transverse component to the displacement magnetic field generated by the time-dependent electric field must be less than  $|\frac{\sigma_c E_{amp} \hbar \omega_Z}{2\gamma}|$ . For <sup>1</sup>H,  $E_{amp} = 10^2 \frac{V}{m}$ , and  $\frac{\omega_Z}{2\pi} = 600$  MHz, this requires that the transverse component of the displacement field must be less than  $1.4 \times 10^{-15}$  T over the detected sample volume. This imposes a strict constraint on the experimental setup used to generate the time-dependent electric field in Eq. (3). For example, if the time-dependent electric field along the  $\hat{y}$ -direction was generated using circular plate capacitors,  $\vec{E}(t) = E_{amp} J_0(\frac{\omega_r r}{c}) \sin(\omega_r t) \hat{y}$ , the magnetic field generated inside the capacitor would be in the  $xz$  plane with a magnitude given by  $|\vec{B}_{disp}(t)| = |\frac{\omega_r r}{2c^2} J_0(\frac{\omega_r r}{c}) E_{amp} \cos(\omega_r t)|$ , where  $r$  is the radius from the center of the circular capacitor plates in the  $xz$  plane,  $c$  is the speed of light, and  $J_n(x)$  is an  $n$ th-order Bessel function of the first-kind. For the transverse component of the displacement magnetic field to be less than the effective field generated by the chiral term in Eq. (5), the sample must be restricted in the  $xz$  plane to an area  $l^2$  such that  $l \ll \frac{\sigma_c c^2}{\gamma}$ , which for <sup>1</sup>H gives the condition that  $l \ll 4.2$  nm. Such a volume restriction renders circular capacitor plates impractical for observing  $\sigma_c$  using a time-dependent electric field.

We propose the experimental setup shown in Fig. 1(a). In this case, a long (infinite) solenoid with an oscillating current,  $I(t) = I_0 \cos(\omega_r t)$ , generates a time-dependent electric field circulating in the  $xy$ -plane along with a time-dependent magnetic field pointing only along the  $\hat{z}$ -direction (a consequence of using an infinite solenoid). For a tightly wound solenoid with  $n$  turns/m and radius of  $a$ , the magnetic and electric fields are given in cylindrical coordinates by<sup>11</sup>

$$\begin{aligned} \vec{B}_{disp}(\vec{r}, t) &= \frac{\pi \omega_r a \mu_0 n I_0 J_1(\frac{\omega_r a}{c})}{2c} \left( J_0\left(\frac{\omega_r r}{c}\right) \sin(\omega_r t) \right. \\ &\quad \left. - N_0\left(\frac{\omega_r r}{c}\right) \cos(\omega_r t) \right) \hat{z}, \\ \vec{E}(\vec{r}, t) &= -\frac{\pi \omega_r a \mu_0 n I_0 J_1(\frac{\omega_r a}{c})}{2} \left( N_1\left(\frac{\omega_r r}{c}\right) \sin(\omega_r t) \right. \\ &\quad \left. + J_1\left(\frac{\omega_r r}{c}\right) \cos(\omega_r t) \right) (\cos(\phi) \hat{y} - \sin(\phi) \hat{x}), \end{aligned} \quad (8)$$

where  $r$  is the radial distance from the center of the solenoid,  $\phi$  is the angular direction with respect to the solenoid axis,  $J_n(x)$  and  $N_n(x)$  are the  $n$ th-order Bessel functions of the first and second-kind, respectively, and  $\mu_0 = 4\pi \times 10^{-7} \frac{V \cdot s}{m \cdot A}$  is the vacuum permeability constant. For  $a = 5$  mm,  $n = 500$  turns/m,  $I_0 = 200$  mA,  $\phi = 0$ ,  $\frac{\omega_r}{2\pi} = 600$  MHz, and with the sample placed a distance  $r = 4$  cm from the central axis of the solenoid, the magnitude of the longitudinal magnetic field is  $|\vec{B}_{disp}| \approx 4 \times 10^{-7}$  T, which for <sup>1</sup>H corresponds to a periodic  $\hat{z}$ -field of  $\frac{\gamma |\vec{B}_{disp}|}{\hbar} \approx 15$  Hz. Since the small longitudinal



magnetic field in Eq. (8) averages to zero on a time scale of  $\frac{2\pi}{\omega_r} = 2$  ns and  $\frac{\gamma|\vec{B}_{\text{disp}}|}{\hbar\omega_r} \ll 1$ , the longitudinal magnetic field generated by the solenoid can be safely neglected in the Bloch equations and consequently has no effect on the steady-state magnetization in Eq. (7) [this conclusion has also been supported from exact integrations of the Bloch equations with an oscillating longitudinal field (data not shown)].

As an example, consider the case of a  $^1\text{H}$  sample in a 600 MHz magnetic field ( $\sigma_c = 2 \times 10^{-18} \frac{\text{m}}{\text{V}}$ ,  $T_1 = T_2 = 1$  s) with dimensions  $5 \text{ mm} \times 5 \text{ mm} \times 1 \text{ cm}$  located a distance of  $r = 4$  cm away from the center of the solenoid with  $a = 5$  mm,  $n = 500$  turns/m,  $I_0 = 200$  mA, and  $\frac{\omega_r}{2\pi} = 600$  MHz and centered in the  $xz$  plane. Using the electric field in Eq. (8),  $\vec{E}(t) \approx (171 \frac{\text{V}}{\text{m}} - 3640 \frac{\text{V}}{\text{m}^2}(x - 0.04 \text{ m})) \sin(\omega_r t) \hat{y} + 28.4 \frac{\text{V}}{\text{m}} \sin(\phi) \cos(\omega_r t) \hat{x}$ , which is predominantly along the  $\hat{y}$  direction. For this configuration, the Hamiltonian in the rotating frame defined by  $\tilde{H}_{INT}(t)$  is given by

$$\begin{aligned} \frac{\tilde{H}_{INT}(r, \phi)}{\hbar} = & \Delta\omega \hat{S}_Z + \frac{\eta\sigma_c\omega_Z}{2} \left( N_1 \left( \frac{\omega_r r}{c} \right) \cos(\phi) \right. \\ & + J_1 \left( \frac{\omega_r r}{c} \right) \sin(\phi) \Big) \hat{S}_Y \\ & + \frac{\eta\sigma_c\omega_Z}{2} \left( J_1 \left( \frac{\omega_r r}{c} \right) \cos(\phi) \right. \\ & \left. - N_1 \left( \frac{\omega_r r}{c} \right) \sin(\phi) \right) \hat{S}_X, \end{aligned} \quad (9)$$

where  $\eta = \frac{\pi\omega_r a \mu_0 n I_0 J_1(\frac{\omega_r a}{c})}{2}$ . Using  $\tilde{H}_{INT}(r, \phi)$  in Eq. (9), the Bloch equations can be solved by considering the spin dynamics within the sample, and the steady-state magnetization will represent an average over the sample volume along with an additional average over the distribution of  $\Delta\omega$  that may be present due to magnetic field inhomogeneity. Simulation of the steady-state transverse magnetization in Figure 2, (right)  $\langle M_{Y,ss} \rangle$  and (left)  $\langle M_{X,ss} \rangle$ , were performed for the sample described above by dividing the sample volume into 1210 small rectangular boxes and by solving the Bloch equations using the effective magnetic field inside each box,  $\tilde{H}_{INT}(r, \phi)$  in Eq. (9). In addition, the results were also averaged over eleven different, equally spaced offsets between  $\Delta\omega = \pm \frac{1}{T_2}$ . In this case, the simulation in Fig. 2 demonstrates that a steady-state is reached in a time  $\tau_{\text{steady-state}} \approx \frac{5T_1T_2}{T_1+T_2}$ , where the sign of the steady-state transverse magnetization depends upon the sign of  $\sigma_c$ . For the simulations,  $\sigma_c = 2 \times 10^{-18} \frac{\text{m}}{\text{V}}$  (green) gave a positive signal, whereas  $\sigma_c = -2 \times 10^{-18} \frac{\text{m}}{\text{V}}$  (blue) gave a negative signal. Note that both  $\langle M_{Y,ss} \rangle$  and  $\langle M_{X,ss} \rangle$  were nonzero in Fig. 2; this was a consequence of the electric field in Eq. (8) having both  $\hat{x}$  and  $\hat{y}$  components. From Fig. 2,  $|\langle M_{Y,ss} \rangle| \approx 8.1 \times 10^{-8} M_{eq}$  and  $|\langle M_{X,ss} \rangle| \approx 4.88 \times 10^{-7} M_{eq}$ , which is the value predicted from Eq. (7) when averaged over  $\Delta\omega$ ,  $|\langle M_{X,ss} \rangle| = 6.45 \times 10^{-7} M_{eq} \langle \frac{1}{1+(\Delta\omega T_2)^2} \rangle = 4.88 \times 10^{-7} M_{eq}$ .

While the above discussion and the simulation results shown in Fig. 2 suggest that an infinite solenoid can be used to generate a chiral signal that is just within the detection limits of liquid-state NMR, an actual experimental implementation of the setup shown in Fig. 1(a) would necessitate using a finite solenoid. In this case, a radial magnetic field would be

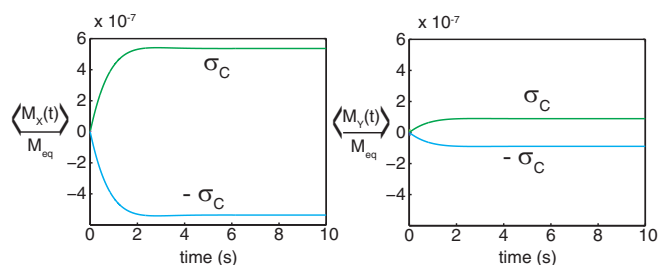


FIG. 2. Simulations of the Bloch equations for the proposed experimental setup in Fig. 1(a): a  $^1\text{H}$  sample [ $T_1 = T_2 = 1$  s,  $\frac{\omega_Z}{2\pi} = 600$  MHz, and  $\sigma_c = 2 \times 10^{-18} \frac{\text{m}}{\text{V}}$  (green) or  $\sigma_c = -2 \times 10^{-18} \frac{\text{m}}{\text{V}}$  (blue)] of dimensions  $5 \text{ mm} \times 5 \text{ mm} \times 1 \text{ cm}$  is placed a distance of  $r = 4$  cm away from the center of solenoid ( $n = 500$  turns/m,  $a = 5$  mm) with a time-dependent current of  $I(t) = 0.2 \text{ A} \cos(\omega_r t)$  where  $\omega_r \approx \omega_Z$  such that  $\Delta\omega \in (-\frac{1}{T_2}, \frac{1}{T_2})$ . The sample was divided up into 1210 smaller volumes, and the effective Hamiltonian in the rotating frame,  $\tilde{H}_{INT}(r, \phi)$  in Eq. (9), was used to integrate the Bloch equations in the various sample regions. The magnetization trajectories were then averaged over the sample volume and over the offset range  $\Delta\omega \in (-\frac{1}{T_2}, \frac{1}{T_2})$ . In the simulations, a steady-state was reached in a time  $\tau_{\text{steady-state}} \approx \frac{5T_1T_2}{T_1+T_2}$ , with  $\langle M_{Y,ss} \rangle \approx \pm 8.1 \times 10^{-8} M_{eq}$  and  $\langle M_{X,ss} \rangle \approx \pm 4.9 \times 10^{-7} M_{eq}$  for  $\sigma_c = \pm 2 \times 10^{-18} \frac{\text{m}}{\text{V}}$ .

present. In order to still use the results from Eq. (7) where the sign of the steady-state transverse magnetization is opposite for different enantiomers, the radial magnetic field generated by the solenoid would need to be less than  $|\frac{\sigma_c \vec{E}(r) \hbar \omega_Z}{2\gamma}|$  over the sample volume. This would require further optimization of the setup in Fig. 1(a) in order to satisfy this constraint in an actual experiment. One possible change to the proposed setup in Fig. 1(a) when using finite solenoids would be to place sample directly between two, identical solenoids with opposite AC currents. To lowest order, the electric fields generated from the two solenoids would add within the sample whereas the radial magnetic fields generated by the two solenoids would cancel at locations equidistant between the two solenoids.

The proposed experimental setup in Fig. 1(a) is also assumed to be placed within the bore of a superconducting magnet. Typical bore sizes are 5.2 cm and 8.9 cm for standard bore and wide bore superconducting magnets, respectively. To readily fit the solenoid and NMR sample within the bore of the magnet may require using either smaller solenoids and/or simply moving the NMR sample closer to the solenoid in Fig. 1(a). Additionally, placing the solenoid inside the bore of magnet could provide an additional source of magnetic field inhomogeneity ( $\Delta\omega$ ) which could slightly affect the magnitude of the steady-state magnetization in Eq. (7) and potentially lead to broader spectra during acquisition. However, the additional magnetic field inhomogeneity generated by placing the solenoid coil within the magnet could likely be compensated for by gradient<sup>14</sup> and/or passive shimming. Alternatively, the solenoid in Fig. 1(a) could be placed above and away from the detection coil. In this case, the NMR sample would be initially placed next to the solenoid coil to generate a steady-state magnetization in Eq. (7), after which the sample would be pneumatically or mechanically shuttled quickly down into a detection coil where the field inhomogeneity would be unaffected by the solenoid coil. These are again

issues that would have to be addressed for any experimental implementation of the proposal presented in this work.

#### IV. CONCLUSIONS

In conclusion, we have proposed using a time-dependent electric field that is periodically modulated at the Larmor frequency in order to detect the pseudoscalar chemical shielding polarizability constant,  $\sigma_c$ , using NMR. This enables NMR to be used to distinguish enantiomers even in achiral environments, since  $(\sigma_c)_L = -(\sigma_c)_R$ . By resonantly modulating the electric field, the chiral term in the NMR Hamiltonian in Eq. (1) appears secular with respect to the dominant Zeeman interaction, thereby enhancing the chiral signal by four to six orders of magnitude over the chiral signal generated using a static electric field. Application of a time-dependent electric field for a time  $\tau_{\text{steady-state}} \approx \frac{5T_1T_2}{T_1+T_2}$ , where  $T_1$  and  $T_2$  are the longitudinal and transverse spin relaxation times, will generate a steady-state transverse magnetization whose sign is opposite for left and right handed enantiomers. Theoretical calculations and numerical simulations using a periodic electric field generated from an infinite solenoid coil with AC current suggest that the chiral signal would be equivalent to the signal from submicromolar concentration of  $^1\text{H}$  nuclei, which is just within the detection limits of liquid-state NMR. For an actual experimental realization of the proposed experiment, the transverse component of magnetic fields must be less than

$|\frac{\sigma \vec{E} \hbar \omega_z}{2\gamma}|$  over the sample volume in order that the chiral contribution dominates and determines the sign of the steady-state magnetization.

#### ACKNOWLEDGMENTS

J.D.W. would like to acknowledge support from the National Science Foundation under Grant No. CHE-1056846 and thank Dr. Stewart Barnes (UM Physics) for helpful discussions on the displacement current and Lauren O'Donnell for a careful reading of the manuscript.

- <sup>1</sup>D. Parker, *Chem. Rev.* **91**, 1441 (1991).
- <sup>2</sup>A. D. Buckingham, *Chem. Phys. Lett.* **398**, 1 (2004).
- <sup>3</sup>R. A. Harris and C. J. Jameson, *J. Chem. Phys.* **124**, 096101 (2006).
- <sup>4</sup>A. D. Buckingham and P. Fischer, *Chem. Phys.* **324**, 111 (2006).
- <sup>5</sup>J. D. Walls, R. A. Harris, and C. J. Jameson, *J. Chem. Phys.* **128**, 154502 (2008).
- <sup>6</sup>A. D. Buckingham, *J. Chem. Phys.* **140**, 011103 (2014).
- <sup>7</sup>G. Monaco and R. Zanasi, *Chirality* **23**, 752 (2011).
- <sup>8</sup>H. Kovacs, D. Moskau, and M. Spraul, *Prog. Nucl. Mag. Res.* **46**, 131 (2005).
- <sup>9</sup>L. Frydman and D. Blazina, *Nat. Phys.* **3**, 415 (2007).
- <sup>10</sup>J. D. Jackson, *Classical Electrodynamics*, 3rd ed. (John Wiley & Sons, Inc., 1998).
- <sup>11</sup>J. D. Templin, *Am. J. Phys.* **63**, 916 (1995).
- <sup>12</sup>P. Lazzeretti, A. Soncini, and R. Zanasi, *Theor. Chem. Acc.* **119**, 99 (2008).
- <sup>13</sup>A. Abragam, *Principles of Nuclear Magnetism* (Oxford University Press Inc., New York, 1983).
- <sup>14</sup>C. A. Michal, *J. Mag. Res.* **185**, 110 (2007).